Ultraheavy atomic dark matter freeze-out through rearrangement

Yu-Cheng Qiu,[1,2,*] Jie Sheng,[1,2,†] Liang Tan,[1,2,‡] and Chuan-Yang Xing[1,2,§]

[1]*Tsung-Dao Lee Institute & School of Physics and Astronomy, Shanghai Jiao Tong University, Shanghai 200240, China*

[2]*Key Laboratory for Particle Astrophysics and Cosmology (MOE) & Shanghai Key Laboratory for Particle Physics and Cosmology, Shanghai Jiao Tong University, Shanghai 200240, China*

(Received 3 January 2024; accepted 19 April 2024; published 10 May 2024)

Atomic dark matter is usually considered to be produced asymmetrically in the early Universe. In this work, we first propose that the symmetric atomic dark matter can be thermally produced through the freeze-out mechanism. The dominant atom antiatom annihilation channel is the atomic rearrangement. It has a geometrical cross section much larger than that of elementary fermions. After the atomic formation, this annihilation process further depletes dark matter particles and finally freezes out. To give the observed dark matter relic, the dark atoms are naturally ultraheavy, ranging from 10^6 to 10^{10} GeV.

DOI: 10.1103/PhysRevD.109.095007

I. INTRODUCTION

More than 80% of the matter in our Universe today is dark matter (DM) [1]. But the nature of DM is still a mystery that suggests new physics beyond the Standard Model (SM) of particle physics [2–4]. Among all DM candidates, the weakly interacting massive particle (WIMP) scenario [5–9] is widely recognized. Its production mechanism, the thermal freeze-out [10,11], is quite natural and attractive. The observed DM density is simply determined by the fundamental parameters, such as the DM mass and its coupling to the SM particles.

However, WIMP predictions have several conflicts with the observations, such as the small scale problems [12,13]. Besides, the DM with a mass of WIMP scale has received strong constraints from direct detection experiments [14–18]. Another appealing candidate, atomic dark matter [19–24], appears as an extension of dark $U(1)$ gauge symmetry. Since dark atom particles are naturally self-interacting, this atomic DM scenario can be utilized to solve the small scale problems [25–31]. In addition, atomic DM also has rich phenomenology in the direct detection [22] and indirect detection [32] experiments.

Being an analogy to the atoms in the SM sector, the atomic DM in the current literature is always designed as asymmetric. Its production is usually considered as the out-of-equilibrium decay of right-handed neutrinos in the early Universe [22,33] as an extension of leptogenesis [34]. The assumption that the production of dark atoms occurs through thermal freeze-out is compelling since it reduces model complexity and provides a rich phenomenology while leaving other possibilities unexplored.

In this work, we first point out that the DM can be symmetric atomic states, which are thermally produced through freeze-out to give the observed relic. The dark sector contains a heavier fermion χ_p and its lighter partner χ_e with opposite dark $U(1)_X$ charges, as well as the same amount of their antiparticles. When the Universe cools down, the dark fermions begin to form atomic bound states. The dark atom mass is dominated by the heavier fermion χ_p, while its radius is determined by the lighter one χ_e [35]. After formation, dark atom and antiatoms annihilate by experiencing an intermediate state of dark positronium and protonium. This is the so-called atomic rearrangement. Its cross section is geometrical and proportional to the atomic size, which is much larger than that of a single fermion, as shown in the cartoon in Fig. 1.[1] Thus, the DM number density is further depleted, and the eventual freeze-out is determined by the atomic rearrangement. As an important result, the symmetric atomic DM scenario naturally produces ultraheavy DM beyond the unitarity bound [38–40].[2]

After introducing such a scenario and its freeze-out history, we explore the viable parameter space. Finally, possible signatures and constraints of the symmetric dark

*ethanqiu@sjtu.edu.cn
†shengjie04@sjtu.edu.cn
‡tanliang@sjtu.edu.cn
§chuan-yang-xing@sjtu.edu.cn

[1]The self-destructing DM has a similar nature that it annihilates after rearrangement [36,37].

[2]Several exquisite mechanisms, such as Refs. [41–45], can also produce ultraheavy or hyperheavy DM thermally.

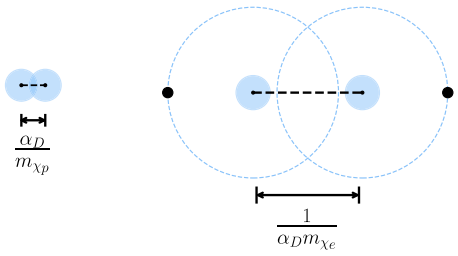

FIG. 1. Illustration of the annihilation cross sections of elementary dark proton, χ_p, and atomic bound state, χ_A (not to scale). The elementary fermions χ_p annihilate when their distance is smaller than $\sim\alpha_D/m_{\chi_p}$, while the dark atoms would rearrange within a distance $\sim 1/\alpha_D m_{\chi_e}$. The latter process is hugely enhanced for $\alpha_D < 1$ and $m_{\chi_p} \gg m_{\chi_e}$.

atom scenario are discussed. Throughout the paper, we use natural units where $c = \hbar = k_B = 1$.

II. SYMMETRIC DARK ATOM SCENARIO

In the dark atom scenario, the dark sector contains a heavier fermion χ_p with mass m_{χ_p} and its lighter partner χ_e with mass m_{χ_e}, as well as their antiparticles $\bar{\chi}_p, \bar{\chi}_e$. χ_p and χ_e interact through a long-range force with opposite charges, which allows the formation of a bound state. Throughout this paper, we take the long-established dark $U(1)_X$ as an example for implementation. The bound atomic state $\chi_A \equiv (\chi_p \chi_e)$ shall form when the temperature is below their binding energy E_b. The subscripts p and e are analogies to the proton and electron in the SM. The dark atom χ_A and its antiparticle account for the DM today.

Our main body Lagrangian is the same as the usual dark atom model [21,22]. However, we do not have the additional assumption of atom-antiatom asymmetry. The Lagrangian is,

$$\mathcal{L} \supset \frac{1}{4}\epsilon F^{\mu\nu}F'_{\mu\nu} - \frac{1}{4}F^{\mu\nu}F_{\mu\nu} - \frac{1}{4}F'^{\mu\nu}F'_{\mu\nu} + \frac{1}{2}m_{A'}^2 A'^{\mu}A'_{\mu} + \bar{\chi}_p(i\not{D} - m_{\chi_p})\chi_p + \bar{\chi}_e(i\not{D} - m_{\chi_e})\chi_e. \tag{1}$$

Here, A' and F' are the dark $U(1)_X$ gauge boson and field strength. As usual, the dark proton χ_p carries $U(1)_X$ charge $+1$ while dark electron χ_e has charge -1. This dark $U(1)_X$ has a mixing with the SM $U(1)_{\rm em}$ by a mixing angle ϵ. The dark gauge boson has a tiny mass to mediate a long-range force and exists as dark radiation. With a mixing satisfying the current limit $\epsilon \lesssim 10^{-12}$ [46,47], the dark sector cannot always be in kinetic equilibrium with the SM sector and will attain its own temperature T_χ. To avoid the big bang nucleosynthesis (BBN) constraint for A', we take $T_\chi = T_{\rm SM}\xi$ and $\xi = 0.2$.[3] Both the dark proton and dark electron maintain in chemical equilibrium inside the dark sector through their annihilation into gauge bosons, $\bar{\chi}_{p(e)} + \chi_{p(e)} \leftrightarrow 2A'$ in the very beginning. The thermal averaged cross section $\langle\sigma_{\rm ann}^{p(e)} v\rangle \simeq \alpha_D^2/m_{\chi_{p(e)}}^2$ is proportional to the square of particle wavelength. Since the dark proton mass is much larger than that of electron and binding energy, χ_p will first freeze out through such a channel, and its yield $Y_{\chi_p} = n_{\chi_p}/s$ stays as a constant for the moment.

As long as the mass of dark $U(1)_X$ gauge boson A' is much smaller than both fermion masses, we can treat the interaction between dark fermions as a Coulomb potential [49], and describe dark atoms by a simple Bohr model with high accuracy. The binding energy and Bohr radius of the dark atom are

$$E_b = \frac{1}{2}\alpha_D^2\mu, \qquad r_b = \frac{1}{\alpha_D\mu}, \tag{2}$$

where dark fine structure constant $\alpha_D \equiv g^2/4\pi$ and reduced mass $\mu \equiv (m_{\chi_p}m_{\chi_e})/(m_{\chi_p} + m_{\chi_e}) \simeq m_{\chi_e}$. With $\alpha_D < 1$, the dark atom size is larger than the Compton wavelength of both χ_p and χ_e.

The dark sector temperature is roughly the kinetic energy of particles inside it. When the Universe cools down to $T_\chi \sim E_b$, the relative kinetic energy between dark protons and electrons becomes smaller than the atomic binding energy. After that, both atom and antiatom begin to form. The atomic formation (AF) cross section is [50],

$$\langle\sigma_{\rm AF}v\rangle = \frac{16\pi}{3\sqrt{3}}\frac{\alpha_D^2}{\mu^2}\left(\frac{E_b}{T_\chi}\right)^{1/2}\ln\left(\frac{E_b}{T_\chi}\right). \tag{3}$$

Symmetry between atom and antiatom indicates that their annihilation also happens once number density accumulates. In the nonrelativistic limit, the annihilation is dominated by the atomic rearrangement (AR) processes [51,52],

$$(\chi_p\chi_e) + (\bar{\chi}_p\bar{\chi}_e) \to (\bar{\chi}_p\chi_p) + \bar{\chi}_e + \chi_e, \tag{4a}$$

$$(\chi_p\chi_e) + (\bar{\chi}_p\bar{\chi}_e) \to (\bar{\chi}_p\chi_p) + (\bar{\chi}_e\chi_e). \tag{4b}$$

The bound states $(\bar{\chi}_p\chi_p)$ and $(\bar{\chi}_e\chi_e)$ shall decay to dark photons subsequently once they are formed. Thus, the atomic annihilation is effectively one directional. In principle, χ_p and $\bar{\chi}_p$ can directly annihilate in flight without forming the intermediate $(\bar{\chi}_p\chi_p)$, but the cross section is usually small compared to the rearrangements [52]. The above processes have a geometrical cross section [51,52],

$$\langle\sigma_{\rm AR}v\rangle \simeq \mathcal{C}\pi r_b^2. \tag{5}$$

The numerical prefactor $\mathcal{C} \sim \mathcal{O}(1)$ could be calculated by investigating the potential between bound states. Generally,

[3]Roughly the extra effective relativistic degree of freedom should be smaller than 0.28 [48] measured from CMB. This translates to a constraint on the temperature ratio, which is $T_\chi < 0.5T_{\rm SM}$ [24].

this factor depends on the collision energy. However, in low-energy regions, this dependence is quite weak [52]. So, we treat it as constant and take $\mathcal{C} = 1$ for both processes.[4] The $\langle \sigma_{\rm AR} v \rangle$ is roughly the geometrical size of the atom. As shown in Fig. 1, before and after the formation of the bound state, the DM size increases by a factor of $\alpha_D^{-4}(m_{\chi_p}/m_{\chi_e})^2$, which significantly enhance the annihilation cross section if $m_{\chi_p} \gg m_{\chi_e}$. The DM annihilation could happen again even with an already depleted density. This further decreases the dark fermion number, and the freeze-out of symmetric dark atoms is then finally determined by atomic rearrangement. As we will see later, the DM mass is ultraheavy, even beyond the unitarity bound, to give the observed relic.

Apart from the processes in Eq. (4), the reaction $\chi_p + (\bar{\chi}_p \bar{\chi}_e) \to (\bar{\chi}_p \chi_p) + \bar{\chi}_e$ and its conjugate reaction occur simultaneously. Their cross sections, denoted as $\sigma_{p\bar{A}}$, are also geometric in nature, with $\sigma_{p\bar{A}} v \simeq \pi r_b^2$. On the other hand, the rearrangement of χ_e and the dark atom is kinetically suppressed at low energy. This is because the binding energy of $(\chi_e \bar{\chi}_e)$ is smaller than that of the dark atom, making the reaction endothermic. As we will discuss later, while the rearrangement annihilation between dark protons and dark atoms leads to a rapid depletion of dark protons once a certain number of dark atoms is produced, the ultimate freeze-out of the dark atom is still primarily determined by the processes described in Eq. (4).

However, the minimal thermal symmetric dark atom model in Eq. (1) has an intrinsic problem. To efficiently consume the dark proton number and convert them into atoms, its lighter partner χ_e should have almost the same yield at the time $T_\chi \sim E_b$. The cross section of dark fermion annihilation into the dark boson is inversely related to its mass square. It means that χ_e has a larger annihilation rate and stays in equilibrium for a longer time. The dark electron has a smaller yield than that of the dark proton when it freezes out. As a result, only a small part of the dark proton can be consumed to form atoms while others are left as millicharged particles. In such case, the atomic annihilation effect becomes negligible, and the heavy dark fermion density shall exceed the total DM density.

One way to solve this problem is to use a real scalar particle ϕ, which can be the real component of dark Higgs from UV completion of $U(1)_X$, with mass $2m_e < m_\phi < 2m_p$. It couples to dark fermions through the Yukawa interaction,[5]

$$\mathcal{L} \supset y_p \phi \bar{\chi}_p \chi_p + y_e \phi \bar{\chi}_e \chi_e. \tag{6}$$

Both Yukawa couplings, y_p and y_e, are small, so that the scalar ϕ does not come into either kinetic or chemical equilibrium with the dark sector. Its merit is to continuously decay to χ_e to help the atomic formation process.

With the model and settings, we are ready to discuss the whole thermal freeze-out history of our symmetric atomic DM scenario.

III. FREEZE-OUT THROUGH ATOMIC REARRANGEMENT

This section shows our scenario naturally introduces a new freeze-out mechanism driven by atomic rearrangement. In the early Universe, the symmetric dark atom scenario has three typical energy scales: the dark proton mass m_{χ_p}, the dark electron mass m_{χ_e}, and binding energy E_b. The unitarity limit of cross section requires the dark coupling to be $\alpha_D \leq 0.5$ [39]. In this paper, the dark proton mass is ultraheavy, and the mass difference between fermions is huge. Thus, there is a hierarchy $m_{\chi_p} \gg m_{\chi_e} \gg E_b$. The whole freeze-out histories of χ_p, χ_e, ϕ, and χ_A have the following clear phases as shown in Fig. 2. Here, the temperature parameter is defined by $x \equiv E_b/T_\chi$, and the parameters are taken as $\alpha_D = 0.2$, $m_{\chi_e} = 1$ GeV, and $\Gamma_\phi = 10^{-24}$ GeV.

A. χ_p Freeze-out ($T_\chi \simeq \mathcal{O}(m_{\chi_p})$)

In this phase, the temperature is so high that all other species remain relativistic and in equilibrium except χ_p. When the dark sector temperature is below m_{χ_p}, the dark proton becomes nonrelativistic and begins to freeze out through the channel $\chi_p + \bar{\chi}_p \leftrightarrow 2A'$. For large $U(1)_X$

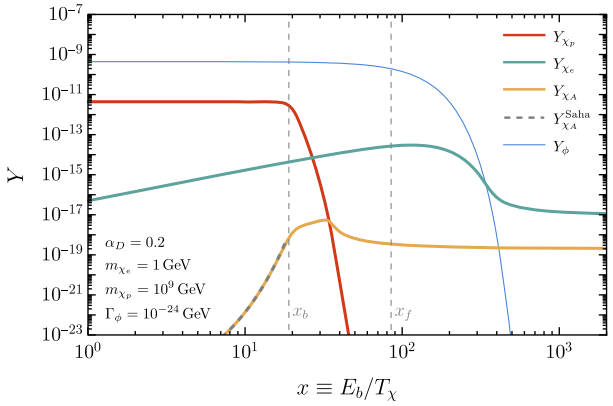

FIG. 2. The yield evolution of dark proton χ_p (red), dark electron χ_e (green), scalar ϕ (blue), and dark atom χ_A (yellow). We take $m_{\chi_e} = 1$ GeV, $\alpha_D = 0.2$, $\Gamma_\phi = 10^{-24}$ GeV, and $Y_\phi^0 = 100 Y_{\chi_p}^0$. The yield of dark atom initially increases due to its formation, then decreases as a result of its rearrangement, and finally freezes out. To achieve the observed relic $\Omega_{\chi_A} h^2 = 0.12$, the dark proton mass is $m_{\chi_p} = 10^9$ GeV. For comparison, the atom yield solution of the Saha equation is drawn as a gray dashed line.

[4]Since cross sections for processes in (4a) and (4b) are both geometrical, they are naturally of the same order. Here we assume that $\mathcal{C} = 1$ for simplicity.

[5]In principle, this scalar can couple to SM Higgs by $\lambda_1 \Lambda \phi H^\dagger H + \lambda_2 \phi^2 H^\dagger H$. However, the interaction should be small to avoid possible constraints from Higgs interaction.

coupling α_D, the Sommerfeld enhancement and the bound-state formation effects should be included in the annihilation cross section, $\langle\sigma^p_{\rm ann}v\rangle = (\alpha_D^2/m^2_{\chi_p})\times\mathcal{S}$, as an effective enhancement factor $\mathcal{S}$ [39]. The dark proton yield after this first stage freeze-out $Y^0_{\chi_p}$ can be fixed by its mass, coupling, and the enhancement factor. Since the χ_p mass is much larger than that of χ_e, this first stage freeze-out temperature $m_{\chi_p}/20$ is far above binding energy E_b. Thus, no dark atom is formed and the yield $Y^0_{\chi_p}$ stays as a constant to give the initial value of the red curve until $T_\chi \sim E_b$. Currently, χ_p with a mass larger than $\mathcal{O}(100)$ TeV is overproduced [38], and the consumption by atomic rearrangement in later phases is necessary.

At the same time, the scalar ϕ gradually freezes in through the channel, $\bar{\chi}_p + \chi_p \to \phi + A'$. Its yield after freeze-in Y^0_ϕ is proportional to the annihilation cross section of order $y_p^2\alpha_D$. It also depends on how long it lasts, $1/T_{fi}$, where the $T_{fi}\sim\mathcal{O}(m_{\chi_p})$ is the endpoint of freeze-in. By integrating the Boltzmann equation of ϕ, one can get

$$Y^0_\phi \simeq 4\times10^{-7}\frac{y_p^2\alpha_D M_P}{g_*^{3/2}T_{fi}}. \tag{7}$$

B. Atomic formation ($T_\chi \gtrsim E_b/x_b \simeq E_b/30$)

When the dark sector temperature cools down to $T_\chi\sim E_b$, the dark electrons begin to pair with the dark protons and form atoms. The density evolution of the dark proton χ_p, dark electron χ_e, and atom state χ_A are described by the following Boltzmann equations with respect to time t:

$$\frac{dY_{\chi_p}}{dt} = -s\langle\sigma_{\rm AF}v\rangle\left(Y_{\chi_p}Y_{\chi_e} - Y^{\rm eq}_{\chi_p}Y^{\rm eq}_{\chi_e}\frac{Y_{\chi_A}}{Y^{\rm eq}_{\chi_A}}\right) - s\langle\sigma_{p\bar{A}}v\rangle Y_{\chi_p}Y_{\chi_A}, \tag{8a}$$

$$\frac{dY_{\chi_e}}{dt} = -s\langle\sigma^e_{\rm ann}v\rangle(Y^2_{\chi_e} - (Y^{\rm eq}_{\chi_e})^2) - s\langle\sigma_{\rm AF}v\rangle\left(Y_{\chi_p}Y_{\chi_e} - Y^{\rm eq}_{\chi_p}Y^{\rm eq}_{\chi_e}\frac{Y_{\chi_A}}{Y^{\rm eq}_{\chi_A}}\right) + \langle\Gamma_\phi\rangle Y_\phi + s\langle\sigma_{\rm AR}v\rangle Y^2_{\chi_A} + s\langle\sigma_{p\bar{A}}v\rangle Y_{\chi_p}Y_{\chi_A}, \tag{8b}$$

$$\frac{dY_{\chi_A}}{dt} = s\langle\sigma_{\rm AF}v\rangle\left(Y_{\chi_p}Y_{\chi_e} - Y^{\rm eq}_{\chi_p}Y^{\rm eq}_{\chi_p}\frac{Y_{\chi_A}}{Y^{\rm eq}_{\chi_A}}\right) - 2s\langle\sigma_{\rm AR}v\rangle Y^2_{\chi_A} - s\langle\sigma_{p\bar{A}}v\rangle Y_{\chi_p}Y_{\chi_A}. \tag{8c}$$

The initial conditions are $Y_{\chi_p(\phi)}|_{T_\chi=E_b} = Y^0_{\chi_p(\phi)}, Y^0_{\chi_A}|_{T_\chi=E_b}=0$. Notice that the inverse process of the atomic rearrangement is neglected. Here, $Y^{\rm eq}_i = n^{\rm eq}_i/s$ and $n^{\rm eq}_i$ is the number density in equilibrium for the corresponding species. The factor 2 in the second term on the right of Eq. (8c) comes from the inclusion of two rearrangement processes [Eq. (4)]. The evolution of antiparticles is the same.

The dark electron χ_e is injected into the Universe all along this phase to pair with dark protons as the green curve. The yield of χ_e is determined by the scalar ϕ decay, $\phi\to\bar{\chi}_e+\chi_e$, and its own annihilation to dark gauge boson including Sommerfeld and bound state formation enhancements. To make sure the χ_e number is large enough, the initial yield of ϕ in Eq. (7) should be larger than the yield of χ_p as $Y^0_\phi \geq Y^0_{\chi_p}$.

On the other hand, dark atoms are constantly being formed and dissociated to maintain in equilibrium. Its evolution can be analytically solved through the Saha equation [53,54] [Eq. (8c) with only atomic formation term since Y_{χ_A} is extremely small compared to Y_{χ_p} in this stage]. The solution,

$$n^{\rm Saha}_{\chi_A} = \frac{n_{\chi_p}n_{\chi_e}}{n^{\rm eq}_{\chi_p}n^{\rm eq}_{\chi_e}}n^{\rm eq}_{\chi_A}, \tag{9}$$

shown as the gray dashed line, perfectly fits the yield evolution of the atom (yellow curve). At this stage, the Y_{χ_p} (red curve) remains constant while the number density of dark atoms increases exponentially, $n^{\rm Saha}_{\chi_A}\propto e^{E_b/T}$.

C. Atomic rearrangement ($T_\chi \gtrsim E_b/x_f \simeq E_b/100$)

As n_{χ_A} accumulates, at the temperature $T_\chi = T_b$ (with $x_b\equiv E_b/T_b$), the rearrangement annihilation of dark proton and dark atoms dominates over the Hubble dilution of n_{χ_p},

$$n_{\chi_A}\langle\sigma_{p\bar{A}}v\rangle > H, \tag{10}$$

where $H(T_{\rm SM}) = 2\sqrt{\pi^3 g_*/45}T^2_{\rm SM}/M_P$ with the Planck mass $M_P\equiv 1/\sqrt{G_N}\approx 1.2\times10^{19}$ GeV. Meanwhile, the atomic formation process is also intense:

$$n_{\chi_e}\langle\sigma_{\rm AF}v\rangle > H. \tag{11}$$

Dark protons, together with dark electrons, quickly form dark atoms and annihilate with antiatoms through atomic rearrangement. So the yield of χ_p drops sharply right after x_b as shown in the red curve.

Shown as the yellow curve, the atomic annihilation also decreases the yield of atom Y_{χ_A}. It becomes more and more difficult for dark atoms to find each other and rearrange. Atomic rearrangement freezes out at the temperature $T_\chi = T_f$ (with $x_f\equiv E_b/T_f$) and Hubble dilution takes over. The eventual freeze-out point is determined by

$$n_{\chi_A}\langle\sigma_{\rm AR}v\rangle \simeq H. \tag{12}$$

The relic of dark atoms makes up the observed DM today. The final dark atom yield $Y^f_{\chi_A}$ is predicted as

$$Y^f_{\chi_A} \simeq \frac{3\sqrt{5}}{\pi^{3/2}\sqrt{g_*}} \frac{m_{\chi_e} x_f \xi}{M_P}. \quad (13)$$

To fit the observed relic $\Omega_{\chi_A} h^2 = 2 m_{\chi_A} s_0 Y^f_{\chi_A} h^2/\rho_c = 0.12$, where $s_0(\rho_c)$ denotes the entropy (critical) density today, the DM mass should be

$$m_{\chi_A} \simeq 10^9 \text{ GeV} \left(\frac{1 \text{ GeV}}{m_{\chi_e}}\right) \left(\frac{g_*}{10}\right)^{1/2} \left(\frac{80}{x_f}\right) \left(\frac{0.2}{\xi}\right). \quad (14)$$

The final yield and DM mass depend simply on the parameter m_{χ_e} and are not sensitive to initial yields before atomic formation. Even the dependence on coupling α_D is canceled out. Besides, the final yield of the atom Y^f_A decreases a lot compared with $Y^0_{\chi_p}$. Thus, the dark proton mass can be lifted to be ultraheavy as 10^9 GeV in the case of Fig. 2.

After all the phases are finished, a large part of ϕ begins to decay, $\Gamma_\phi \simeq y_e^2 m_\phi/4\pi \simeq H(E_b/x_f\xi)$. Without ϕ injection, the dark electron will finally annihilate and freeze out. Since the mass difference is huge, $m_{\chi_e} \ll m_{\chi_p} \approx m_{\chi_A}$, the millicharged dark electron only accounts for a tiny portion of DM.

So far, we have seen the key points of the symmetric dark atom scenario. Its freeze-out is determined by atomic rearrangement and can give the observed relic. Since the geometric cross section of atom annihilation is much larger than the annihilation cross section of χ_p itself as a pointlike particle, the number density of dark sector particles is greatly suppressed, and its mass is enhanced to be ultraheavy.

IV. PARAMETER SPACE AND CONSTRAINTS

We first explore the required parameter space of ϕ to make the symmetric atomic DM scenario work. (i) We expect the decay of ϕ to happen after the freeze-out of the dark atom, $\Gamma_\phi < H(x_f)$. Otherwise, the injection of χ_e during atomic formation is not sufficient and χ_p cannot be significantly depleted. (ii) Since ϕ is produced by freeze-in and never enters equilibrium, its yield after freeze-in should be smaller than its relativistic equilibrium yield, $Y^0_\phi < T^3_\chi/\pi^2 s \simeq 0.0018\ g_*^{-1}$. (iii) The yield of χ_e before x_b is controlled by two major processes, its self-annihilation and the decay of ϕ. The depletion of χ_e due to its self-annihilation should be compensated for by the production from the decay of ϕ. Its yield is approximately $Y_{\chi e} \approx \sqrt{\Gamma_\phi Y^0_\phi / s\langle\sigma^e_{\rm ann} v\rangle}$. To meet the criterion of the minimal number density of χ_e as Eq. (11), one obtains another requirement for ϕ, which is $\Gamma_\phi Y^0_\phi > H(x_b)^2 \langle\sigma^e_{\rm ann} v\rangle / s\langle\sigma_{\rm AF} v\rangle^2$. In Fig. 3, we show the allowed parameter space (blank area) that satisfies these three conditions for ϕ by taking $\alpha_D = 0.2$ and $m_{\chi_p} = 10^9$ GeV.

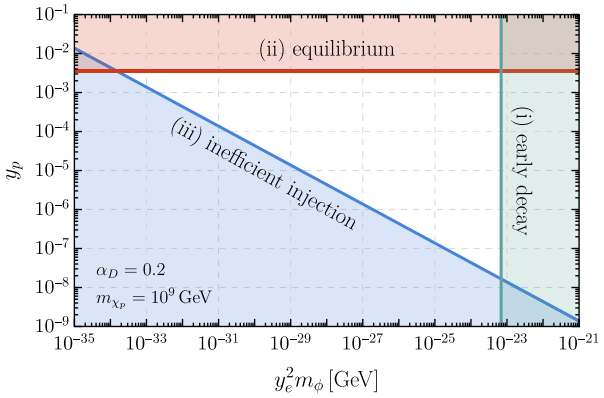

FIG. 3. The parameter space for ϕ in the $(y_e^2 m_\phi, y_p)$ plane that successfully initiates the thermal freeze-out of the symmetric dark atom. Here we take $\alpha_D = 0.2$ and $m_{\chi_p} = 10^9$ GeV.

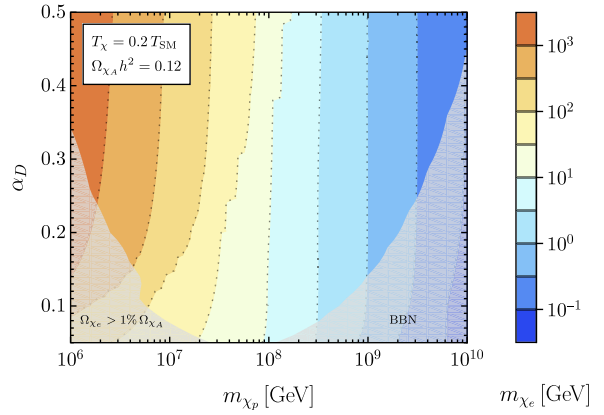

FIG. 4. The parameter space where dark atom is giving the observed DM relic $\Omega_{\chi_A} h^2 = 0.12$. The horizontal axis is the DM mass $m_{\chi_A} \approx m_{\chi_p}$, and the vertical axis is the coupling α_D. Different colors stand for different values of dark electron mass m_{χ_e}. The DM mass is not sensitive to the coupling but inversely proportional to dark electron mass. The gray shaded area is excluded by the BBN constraint and the overproduction of χ_e, $\Omega_{\chi_e} > 1\%\Omega_{\chi_A}$.

The parameter space of the symmetric atomic DM to give the correct DM relic $\Omega_{\chi_A} h^2 = 0.12$ is shown in Fig. 4. Here, we fix the scalar yield after its freeze-in as $Y^0_\phi = 100 \times Y^0_{\chi_p}$, and it decays around $x = E_b/T_\chi \sim 100$ by choosing appropriate y_p, y_e, and m_ϕ. Once the above conditions are met, the impact of different parameter values of ϕ on the dark atom abundance becomes negligible. The DM relic then depends on three parameters, dark fermion masses m_{χ_p}, m_{χ_e}, and the dark $U(1)_X$ coupling α_D. One can see that the DM mass $m_{\chi_A} \approx m_{\chi_p}$ can be in the range of $(10^6, 10^{10})$ GeV by varying $\alpha \subset (0.05, 0.5)$ and $m_{\chi_e} \subset (10^{-1}, 10^3)$ GeV. Exactly as expected in Eq. (14), the DM mass $m_{\chi_A}(m_{\chi_p})$ is not sensitive to coupling α_D but

inversely proportional to the dark electron mass m_{χ_e}. The reason is as follows. A lighter dark electron leads to a larger atomic rearrangement cross section. The dark atom yield becomes smaller after its freeze-out. As a result, the DM shall be heavier to give the correct relic.

The parameters in the bottom-left corner of the figure lead to an overproduction of χ_e by the criterion $\Omega_{\chi_e} > 1\%\Omega_{\chi_A}$. For a larger m_{χ_e} and a smaller α_D, the annihilation cross section of dark electron is suppressed. Thus, more dark electrons are left as relic. The region where the dark fermions have a small mass difference is disfavored. It indicates that the freeze-out through atomic rearrangement naturally produces DM heavier than the unitarity bound.

If the binding energy $E_b \propto \alpha_D^2 m_e$ is too small, the atomic formation and annihilation happen around the BBN epoch. The number and energy density of χ_p before consumption can be large enough to affect BBN. Thus, the bottom-right corner is excluded as shown by the gray shaded area.

V. CONCLUSION AND DISCUSSION

In this paper, we propose a new scenario in which DM is composed of both dark atoms and antiatoms symmetrically and discuss its freeze-out production. In this scenario, a heavier dark fermion χ_p pairs with a lighter partner χ_e to form an atomic state. Since the cross section of atomic annihilation through rearrangement is much larger than the unitarity limit of χ_p annihilation, the dark sector particles are further consumed after atomic formation. The dark atom freeze-out is determined by their rearrangements. Notably, the mass of DM can avoid the unitarity bound and be lifted to $\mathcal{O}(10^{10})$ GeV.

About the possible signatures of the symmetric dark atom scenario, we have the following open discussions. Compared with the asymmetric dark atom scenario, the symmetric case has different phenomena for the annihilation between particle and antiparticle appears. This annihilation can be tested through indirect detection and cosmological observation. Usually, such constraints are not sensitive to heavy DM because of the small number density [55,56]. However, the large annihilation cross section of the symmetric DM is a remedy for this deficiency. The ultraheavy symmetric atomic DM is self-interacting with a huge cross section. Thus, its halo density profile could be different from those of other models. This difference also imprints in the matter power spectrum at small scales. Furthermore, the annihilation of atomic DM shall distort cosmic microwave background (CMB) and leave indirect detection signals today. These phenomenological research studies will be explored in future works.

ACKNOWLEDGMENTS

The authors thank Yu Cheng and Chen Xia for useful discussions. Jie Sheng deeply thanks Professor Shao-Feng Ge, Tsutomu Yanagida san, and Mengfan Shi for their encouragement. This work is supported by the National Natural Science Foundation of China (12247141, 12247148, 12375101, 12090060, 12090064) and the SJTU Double First Class start-up fund (WF220442604).

[1] N. Aghanim *et al.* (Planck Collaboration), Planck 2018 results. VI. Cosmological parameters, Astron. Astrophys. **641**, A6 (2020); **652**, C4(E) (2021).
[2] Gianfranco Bertone, Dan Hooper, and Joseph Silk, Particle dark matter: Evidence, candidates and constraints, Phys. Rep. **405**, 279 (2005).
[3] Bing-Lin Young, A survey of dark matter and related topics in cosmology, Front. Phys. (Beijing) **12**, 121201 (2017); **12**, 121202(E) (2017).
[4] A. Arbey and F. Mahmoudi, Dark matter and the early Universe: A review, Prog. Part. Nucl. Phys. **119**, 103865 (2021).
[5] Gary Steigman and Michael S. Turner, Cosmological constraints on the properties of weakly interacting massive particles, Nucl. Phys. **B253**, 375 (1985).
[6] Mark W. Goodman and Edward Witten, Detectability of certain dark matter candidates, Phys. Rev. D **31**, 3059 (1985).
[7] Gerard Jungman, Marc Kamionkowski, and Kim Griest, Supersymmetric dark matter, Phys. Rep. **267**, 195 (1996).
[8] Giorgio Arcadi, Maíra Dutra, Pradipta Ghosh, Manfred Lindner, Yann Mambrini, Mathias Pierre, Stefano Profumo, and Farinaldo S. Queiroz, The waning of the WIMP? A review of models, searches, and constraints, Eur. Phys. J. C **78**, 203 (2018).
[9] Leszek Roszkowski, Enrico Maria Sessolo, and Sebastian Trojanowski, WIMP dark matter candidates and searches—current status and future prospects, Rep. Prog. Phys. **81**, 066201 (2018).
[10] Benjamin W. Lee and Steven Weinberg, Cosmological lower bound on heavy neutrino masses, Phys. Rev. Lett. **39**, 165 (1977).
[11] Edward W. Kolb and Michael S. Turner, *The Early Universe* (CRC Press, Boca Raton, 1990), Vol. 69.
[12] Mark Vogelsberger, Jesus Zavala, Francis-Yan Cyr-Racine, Christoph Pfrommer, Torsten Bringmann, and Kris Sigurdson, ETHOS—An effective theory of structure formation: Dark matter physics as a possible explanation of the small-scale CDM problems, Mon. Not. R. Astron. Soc. **460**, 1399 (2016).

[13] James S. Bullock and Michael Boylan-Kolchin, Small-scale challenges to the ΛCDM paradigm, Annu. Rev. Astron. Astrophys. **55**, 343 (2017).
[14] Marc Schumann, Direct detection of WIMP dark matter: Concepts and status, J. Phys. G **46**, 103003 (2019).
[15] Yue Meng *et al.* (PandaX-4T Collaboration), Dark matter search results from the PandaX-4T commissioning run, Phys. Rev. Lett. **127**, 261802 (2021).
[16] D. S. Akerib *et al.*, Snowmass2021 cosmic frontier dark matter direct detection to the neutrino fog, in Snowmass 2021 (2022), arXiv:2203.08084.
[17] J. Aalbers *et al.* (LZ Collaboration), First dark matter search results from the LUX-ZEPLIN (LZ) experiment, Phys. Rev. Lett. **131**, 041002 (2023).
[18] E. Aprile *et al.* (XENON Collaboration), First dark matter search with nuclear recoils from the XENONnT experiment, Phys. Rev. Lett. **131**, 041003 (2023).
[19] S. I. Blinnikov and M. Y. Khlopov, Possible astronomical effects of mirror particles, Astron. Zh. **60**, 632 (1983).
[20] Haim Goldberg and Lawrence J. Hall, A new candidate for dark matter, Phys. Lett. B **174**, 151 (1986).
[21] David E. Kaplan, Gordan Z. Krnjaic, Keith R. Rehermann, and Christopher M. Wells, Atomic dark matter, J. Cosmol. Astropart. Phys. 05 (2010) 021.
[22] David E. Kaplan, Gordan Z. Krnjaic, Keith R. Rehermann, and Christopher M. Wells, Dark atoms: Asymmetry and direct detection, J. Cosmol. Astropart. Phys. 10 (2011) 011.
[23] James M. Cline, Zuowei Liu, and Wei Xue, Millicharged atomic dark matter, Phys. Rev. D **85**, 101302 (2012).
[24] James M. Cline, Dark atoms and composite dark matter, SciPost Phys. Lect. Notes **52**, 1 (2022).
[25] Francis-Yan Cyr-Racine and Kris Sigurdson, Cosmology of atomic dark matter, Phys. Rev. D **87**, 103515 (2013).
[26] James M. Cline, Zuowei Liu, Guy Moore, and Wei Xue, Scattering properties of dark atoms and molecules, Phys. Rev. D **89**, 043514 (2014).
[27] Kalliopi Petraki, Lauren Pearce, and Alexander Kusenko, Self-interacting asymmetric dark matter coupled to a light massive dark photon, J. Cosmol. Astropart. Phys. 07 (2014) 039.
[28] Kimberly K. Boddy, Manoj Kaplinghat, Anna Kwa, and Annika H. G. Peter, Hidden sector hydrogen as dark matter: Small-scale structure formation predictions and the importance of hyperfine interactions, Phys. Rev. D **94**, 123017 (2016).
[29] Prateek Agrawal, Francis-Yan Cyr-Racine, Lisa Randall, and Jakub Scholtz, Dark catalysis, J. Cosmol. Astropart. Phys. 08 (2017) 021.
[30] Sean Tulin and Hai-Bo Yu, Dark matter self-interactions and small scale structure, Phys. Rep. **730**, 1 (2018).
[31] Saurabh Bansal, Jared Barron, David Curtin, and Yuhsin Tsai, Precision cosmological constraints on atomic dark matter, J. High Energy Phys. 10 (2023) 095.
[32] Lauren Pearce, Kalliopi Petraki, and Alexander Kusenko, Signals from dark atom formation in halos, Phys. Rev. D **91**, 083532 (2015).
[33] Jeremie Choquette and James M. Cline, Minimal non-Abelian model of atomic dark matter, Phys. Rev. D **92**, 115011 (2015).
[34] M. Fukugita and T. Yanagida, Baryogenesis without grand unification, Phys. Lett. B **174**, 45 (1986).
[35] J Sakurai and J Napolitano, *Modern Quantum Mechanics*, 2 ed. (Person New International edition, Boston, 2014), p. 39.
[36] Michael Geller and Ofri Telem, Self-destructing atomic dark matter, Phys. Rev. D **104**, 035010 (2021).
[37] Yuval Grossman, Roni Harnik, Ofri Telem, and Yue Zhang, Self-destructing dark matter, J. High Energy Phys. 07 (2019) 017.
[38] Kim Griest and Marc Kamionkowski, Unitarity limits on the mass and radius of dark matter particles, Phys. Rev. Lett. **64**, 615 (1990).
[39] Benedict von Harling and Kalliopi Petraki, Bound-state formation for thermal relic dark matter and unitarity, J. Cosmol. Astropart. Phys. 12 (**2014**) 033.
[40] Juri Smirnov and John F. Beacom, TeV-scale thermal WIMPs: Unitarity and its consequences, Phys. Rev. D **100**, 043029 (2019).
[41] Keisuke Harigaya, Masahiro Ibe, Kunio Kaneta, Wakutaka Nakano, and Motoo Suzuki, Thermal relic dark matter beyond the unitarity limit, J. High Energy Phys. 08 (2016) 151.
[42] Asher Berlin, WIMPs with GUTs: Dark matter coannihilation with a lighter species, Phys. Rev. Lett. **119**, 121801 (2017).
[43] Hyungjin Kim and Eric Kuflik, Superheavy thermal dark matter, Phys. Rev. Lett. **123**, 191801 (2019).
[44] Eric David Kramer, Eric Kuflik, Noam Levi, Nadav Joseph Outmezguine, and Joshua T. Ruderman, Heavy thermal dark matter from a new collision mechanism, Phys. Rev. Lett. **126**, 081802 (2021).
[45] Ronny Frumkin, Eric Kuflik, Itay Lavie, and Tal Silverwater, Roadmap to thermal dark matter beyond the weakly interacting dark matter unitarity bound, Phys. Rev. Lett. **130**, 171001 (2023).
[46] Matthias Schwarz, Ernst-Axel Knabbe, Axel Lindner, Javier Redondo, Andreas Ringwald, Magnus Schneide, Jaroslaw Susol, and Günter Wiedemann, Results from the solar hidden photon search (SHIPS), J. Cosmol. Astropart. Phys. 08 (2015) 011.
[47] Andrea Caputo, Ciaran A. J. O'Hare, Alexander J. Millar, and Edoardo Vitagliano, Dark photon limits: A cookbook, Phys. Rev. D **104**, 095029 (2021).
[48] R. L. Workman *et al.* (Particle Data Group), Review of particle physics, Prog. Theor. Exp. Phys. **2022**, 083C01 (2022).
[49] M. Napsuciale and S. Rodriguez, Complete analytical solution to the quantum Yukawa potential, Phys. Lett. B **816**, 136218 (2021).
[50] Igor' Il'ich Sobel'Man, *Introduction to the Theory of Atomic Spectra: International Series of Monographs in Natural Philosophy* (Elsevier, New York, 2016), Vol. 40.
[51] David L. Morgan and Vernon W. Hughes, Atom-antiatom interactions, Phys. Rev. A **7**, 1811 (1973).
[52] Piotr Froelich, Svante Jonsell, Alejandro Saenz, Bernard Zygelman, and Alex Dalgarno, Hydrogen-antihydrogen collisions, Phys. Rev. Lett. **84**, 4577 (2000).
[53] Megh Nad Saha, LIII. Ionization in the solar chromosphere, Philos. Mag. **40**, 472 (1920).
[54] Meghnad N. Saha, On a physical theory of stellar spectra, Proc. R. Soc. Ser. A **99**, 135 (1921).

[55] Gilly Elor, Nicholas L. Rodd, Tracy R. Slatyer, and Wei Xue, Model-independent indirect detection constraints on hidden sector dark matter, J. Cosmol. Astropart. Phys. 06 (2016) 024.

[56] Masahiro Kawasaki, Hiromasa Nakatsuka, Kazunori Nakayama, and Toyokazu Sekiguchi, Revisiting CMB constraints on dark matter annihilation, J. Cosmol. Astropart. Phys. 12 (2021) 015.